

Observation of Mean-Spin Barrier Bump in Sub-Barrier Fusion of ^{28}Si with ^{154}Sm

S. Gil, D. Abriola, D. E. DiGregorio, M. di Tada, M. Elgue, A. Etchegoyen, M. C. Etchegoyen, J. Fernández Niello, A. M. J. Ferrero, A. O. Macchiavelli, A. J. Pacheco, J. E. Testoni, P. Silveira Gomes,^(a) and V. R. Vanin^(b)

Laboratorio Tandem, Comisión Nacional de Energía Atómica, Buenos Aires, Argentina

A. Charlop, A. García, S. Kailas,^(c) S. J. Luke, E. Renshaw,^(d) and R. Vandenbosch
Nuclear Physics Laboratory, University of Washington, Seattle, Washington 98195

(Received 17 August 1990)

We have measured the fusion excitation function and γ -ray multiplicities M_γ for the $^{28}\text{Si} + ^{154}\text{Sm}$ system. We have also measured M_γ for the $^{16}\text{O} + ^{166}\text{Er}$ system that leads to the same compound nucleus, ^{182}Os , as a calibration of the connection between M_γ and the first moment of the spin distribution, $\langle I \rangle$. We find that the deduced $\langle I \rangle$ for $^{28}\text{Si} + ^{154}\text{Sm}$ agrees reasonably well with theoretical calculations, and in particular its energy dependence exhibits the barrier bump expected when a shape degree of freedom is strongly coupled to the relative motion.

PACS numbers: 25.70.Jj, 25.70.Gh, 27.70.+q

Fusion of heavy ions at low bombarding energies is governed largely by the quantum-mechanical penetration through the Coulomb plus centrifugal barrier. Fusion cross-section excitation functions have been measured for many heavy-ion systems, and are observed to become orders of magnitude larger than one-dimensional barrier-penetration calculations at the lowest observable energies. These enhancements are understood in terms of theoretical models which explicitly consider the coupling of the relative-motion coordinate in the entrance channel to other degrees of freedom (deformation, vibration, and transfer).^{1,2} Thus sub-barrier fusion is an interesting process for probing the role of several degrees of freedom in quantum-mechanical tunneling processes. However, a more stringent test can be obtained by comparing not only the fusion cross section but also the shape of the spin distribution which comprises the fusion cross section.

Information on the first moment of the spin distribution, $\langle I \rangle$, can be obtained from measurement of average γ -ray multiplicities M_γ .³⁻⁵ Higher moments can, in principle, be deduced by measuring full multiplicity distributions with large-array γ detectors.^{6,7} Recently, $\langle I \rangle$ has been determined from measurements of the ratio of the population of a high-spin isomer state to that of a low-spin ground state.^{8,9} The second moment of the spin distributions can be obtained from measurements of α or fission-fragment angular anisotropies.^{10,11}

One-dimensional barrier-penetration models predict that the first moment of the spin distribution should decrease more slowly with decreasing bombarding energy as one approaches the barrier, and eventually reach an approximately constant but nonzero value at sub-barrier energies.¹² This saturation effect of $\langle I \rangle$ at energies below the Coulomb barrier has been observed recently for $^{12}\text{C} + ^{128}\text{Te}$, $^7\text{Li} + ^{133}\text{Cs}$, and $^3\text{He} + ^{136}\text{Ba}$,^{8,9} where the coupling to the shape degrees of freedom is relatively

weak. If the coupling to other degrees of freedom, such as shape degrees of freedom, is strong, then $\langle I \rangle$ increases in the vicinity of the barrier. This gives rise to a bump in the energy dependence of $\langle I \rangle$ relative to the no-coupling case.¹² Although increases in $\langle I \rangle$ have been observed at low bombarding energies,^{5,6,12} the predicted energy dependence has not been clearly established experimentally, largely because of the difficulties in obtaining information at sub-barrier energies where the cross section is small.

In the present work we have exploited the sensitivity of an electrostatic deflector to measure γ -ray multiplicities as a probe of the spin distribution in the $^{28}\text{Si} + ^{154}\text{Sm}$ system. Traditionally the connection between the measured γ -ray multiplicities and $\langle I \rangle$ has been made through the systematic relation between these quantities in neighboring regions of the periodic table³ or through *a priori* expectations for this relation.⁶ In a previous work³ we have shown that above the barrier, and in particular for more asymmetric systems, the experimental values of $\langle I \rangle$ agree with almost any theoretical model, including the sharp-cutoff approximation, that correctly describes the fusion cross section. In the present study we determined the M_γ vs $\langle I \rangle$ "calibration" experimentally by using the reaction $^{16}\text{O} + ^{166}\text{Er}$ that leads to the same compound nucleus ^{182}Os . At bombarding energies between 75 and 100 MeV this reaction spans the same range of excitation energies and angular momentum (multiplicities) as the reaction $^{28}\text{Si} + ^{154}\text{Sm}$ at bombarding energies between 107 and 144 MeV, as can be seen by comparing Figs. 1(b) and 2(b). The relevant energy range spanned by the $^{16}\text{O} + ^{166}\text{Er}$ reaction lies above the Coulomb barrier for this system, where, as mentioned above, the spin distribution becomes relatively model independent once the fusion cross section is reproduced. (For example, the $\langle I \rangle$ values from sharp-cutoff and coupled-channel models differ by less than 5% at a bombarding energy of 80

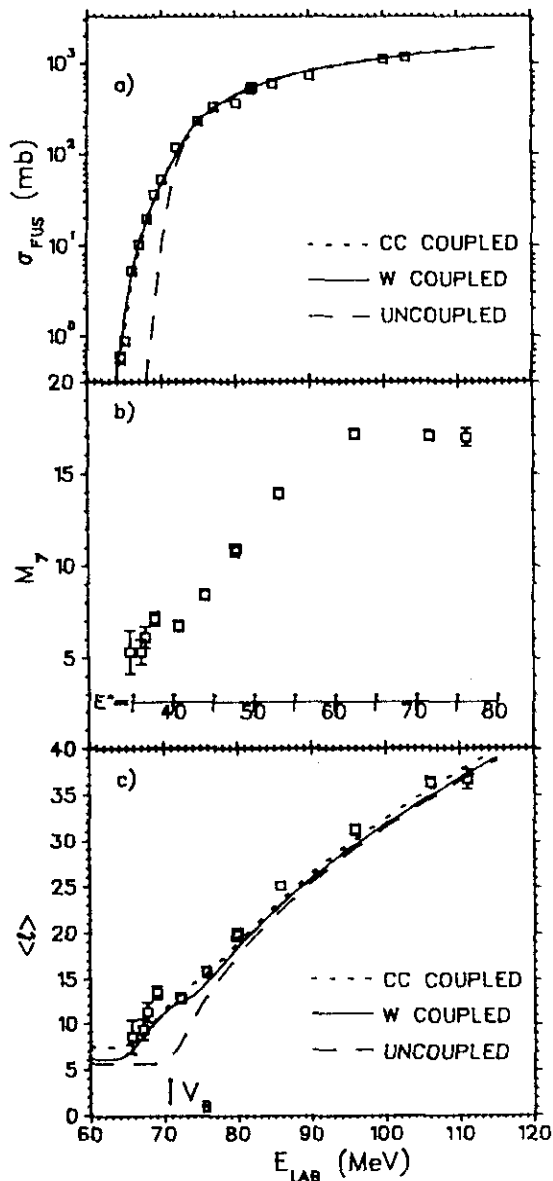


FIG. 1. $^{16}\text{O} + ^{166}\text{Er}$. (a) Fusion excitation function (Ref. 14). The solid curve is a fit to the data using the Wong model ($V_b = 64.5$ MeV, $R_b = 11.06$ fm, $\hbar\omega = 3.40$ MeV, $\beta_2 R = 0.23 \times 6.58 = 1.5$ fm). The dashed curve is the same fit with the coupling turned off. The dotted curve is from a coupled-channel calculation ($V_b = 65.3$ MeV c.m., $R_b = 11.27$ fm, $\hbar\omega = 4.61$ MeV) including the static deformation ($\beta_2 R = 0.342 \times 6.60 = 2.26$ fm) and the octupole vibration ($\beta_3 R = 0.053 \times 6.60 = 0.35$ fm). (b) Experimental γ -ray multiplicities as a function of laboratory energy. Excitation energies E^* of the compound nucleus ^{182}Os are also shown. (c) Experimental $\langle I \rangle$ obtained from multiplicities. The solid and dotted curves are predictions from the Wong-model and the coupled-channel calculations described above. The dashed curve is from the Wong model without coupling.

MeV.)

Measurements were made using both the tandem accelerator at the Tandem Laboratory and the tandem-booster accelerator at the University of Washington.

The measurements of the $^{28}\text{Si} + ^{154}\text{Sm}$ fusion cross sections were performed at the Tandem Laboratory using the delayed-x-ray-activity technique discussed in Ref. 13. The half-lives and the number of x rays produced per decay are of course the same as those used in the $^{16}\text{O} + ^{166}\text{Er}$ reaction, since both reactions lead to the same residual nuclei.¹⁴ The experimental fusion cross sections for $^{28}\text{Si} + ^{154}\text{Sm}$ are presented in Fig. 2(a) (squares) as a function of laboratory bombarding energy. We have also made an independent measurement of the fusion cross section at several energies by measuring the absolute intensities of the rotational deexcitations in the $4n$ channel product ^{178}Os . When these intensities are extrapolated to $J = 0$ and corrected for the fraction of the fusion cross section leading to the $4n$ channel, they give rise to cross sections in good agreement with those obtained by the delayed-x-ray-activity method [see plus symbols in Fig. 2(a)].

The γ multiplicities were obtained using the electrostatic deflector at the University of Washington Nuclear Physics Laboratory.⁵ Since the fusion products are strongly peaked at zero degrees, high efficiency can be achieved with this device. The electrostatic deflector was used in combination with two $7.6 \text{ cm} \times 7.6 \text{ cm}$ NaI detectors and a low-pressure multiwire proportional counter (Breskin detector).¹⁵ The Breskin counter, in conjunction with the time signal from the pulsed beam, provided the time of flight of the particles. This information enabled us to separate the evaporation-residue fusion products from the quasielastic events. The ratio of these residues in coincidence with the NaI detectors to the residue singles yields M_γ , independent of the efficiency of the Breskin detector. The present experimental technique is discussed in detail elsewhere.¹⁶ The results of our multiplicity measurements for $^{16}\text{O} + ^{166}\text{Er}$ and $^{28}\text{Si} + ^{154}\text{Sm}$ are shown in Figs. 1(b) and 2(b). The values of M_γ reported here have not been corrected for internal conversion. This correction is included, however, in the determination of $\langle I \rangle$ and is the same for both of the systems studied here.

The fusion cross-section excitation function for the $^{16}\text{O} + ^{166}\text{Er}$ system has been measured recently,¹⁴ and is shown in Fig. 1(a). The fusion excitation function has been fitted by the Wong model¹⁷ which takes into account the quadrupole deformation of the target, and by a coupled-channel model¹⁸ where we can include both the projectile and target quadrupole deformations and also the target hexadecapole deformation and octupole vibration. We show the expectation of these two models for $\langle I \rangle$ in Fig. 1(c). Above the barrier V_b , both models agree fairly well, with the difference among them giving an estimate of the uncertainty in the value of $\langle I \rangle$ at each energy. The connection between the measured M_γ and $\langle I \rangle$ was made using the procedure of Halbert *et al.*⁶ The results for the $^{16}\text{O} + ^{166}\text{Er}$ system in Fig. 1(c) thus serve as a calibration of this procedure. Then we use this procedure for obtaining $\langle I \rangle$ from M_γ for the $^{28}\text{Si} + ^{154}\text{Sm}$

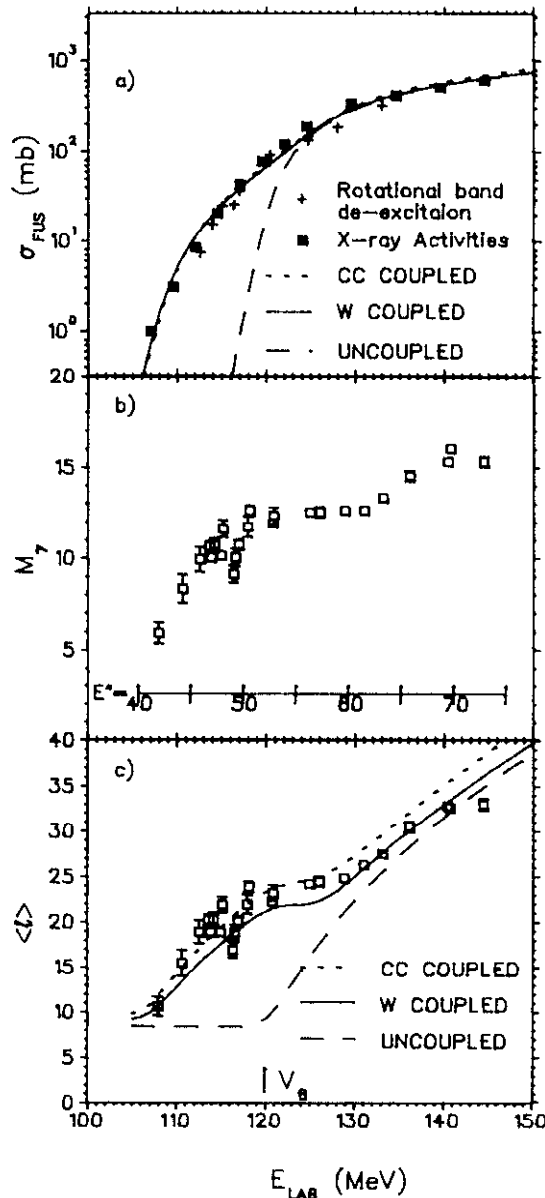


FIG. 2. $^{28}\text{Si} + ^{154}\text{Sm}$. (a) Fusion excitation functions from x-ray activities and rotational-band deexcitation of $^{154}\text{Sm}(^{28}\text{Si}, 4n)^{178}\text{Os}$. The solid curve is a fit to the data using the Wong model ($V_b = 101.5$ MeV c.m., $R_b = 10.91$ fm, $\hbar\omega = 4.55$ MeV, $\beta_2 R = 0.24 \times 6.43 = 1.54$ fm). The dashed curve is the same fit with the coupling turned off. The dotted curve is a coupled-channel calculation ($V_b = 102.2$ MeV c.m., $R_b = 11.48$ fm, $\hbar\omega = 4.3$ MeV) including the static deformation of ^{154}Sm ($\beta_2 R = 0.341 \times 6.43 = 2.19$ fm, $\beta_4 R = 0.07 \times 6.43 = 0.45$ fm), the octupole vibration of ^{154}Sm ($\beta_3 R = 0.1 \times 6.43 = 0.64$ fm), and the quadrupole vibration of ^{28}Si ($\beta_2 R = -0.41 \times 3.42 = -1.37$ fm). (b) Experimental γ multiplicities. Excitation energies of the compound nucleus ^{182}Os are also shown. (c) Experimental $\langle l \rangle$ from multiplicities. The solid and dotted curves are predictions from the Wong-model and the coupled-channel calculations described above. The dashed curve is from the Wong model without coupling.

system at excitation energies between 42 and 74 MeV. The results are shown in Fig. 2(c).

As in the case of the $^{16}\text{O} + ^{166}\text{Er}$ calibration reaction, we have fitted the fusion excitation function for $^{28}\text{Si} + ^{154}\text{Sm}$ with the same models as mentioned above. The parameters used are given in the figure caption. We then show in Fig. 2(c) the expected $\langle l \rangle$ from these models. It can be seen that the coupling effects are very strong, leading to a large increase in the $\langle l \rangle$ values near the barrier. It is also seen that our measurements are in accord with this expectation, demonstrating clearly the expected effect. The quadrupole deformation of ^{154}Sm is the dominant contributor to the coupling effects. The consistency of the $\langle l \rangle$ values with the shape of the excitation function, as well as the observation that $\langle l \rangle$ returns close to the expected no-coupling limit at the lowest bombarding energy, gives confidence that the basic assumptions in the barrier penetration process are correct. In particular, it suggests that the inertial mass of the system can be approximated by its reduced mass at least for this relatively mass-asymmetric entrance channel.¹⁹

It is perhaps useful at this point to recall the physical origin of the increase in $\langle l \rangle$ at near-barrier energies. Depending on the relative orientation of the deformed reaction partners, the $l=0$ barrier is either raised or lowered compared to that for spherical reaction partners. At bombarding energies near the $l=0$ barrier a lowering of the barrier allows many more partial waves to contribute than would otherwise be possible, increasing the $\langle l \rangle$ dramatically. The difference in the magnitude of the bump between the two systems studied here can be understood in terms of the reduced masses involved. In the case of the $^{28}\text{Si} + ^{154}\text{Sm}$ system, the spacing between the effective potential for the adjacent l 's is less than for the $^{16}\text{O} + ^{166}\text{Er}$ system. Therefore, for similar values of the strength of the coupling to deformation degrees of freedom, the increase in $\langle l \rangle$ is larger in the former system, as seen in Figs. 1(c) and 2(c). At very sub-barrier energies one is below the barrier for all orientations, and the l distribution is determined by the relative penetrabilities of the different l -dependent barriers which for parabolic barriers are independent of energy when $E \ll V_b$. At energies well above the barrier many l values are already above barrier, and fluctuations in the $l=0$ barrier affects a smaller fraction of the contributing partial waves and $\langle l \rangle$ approaches the no-coupling limit at high E .

In summary, we have measured the average γ -ray multiplicities for the $^{16}\text{O} + ^{166}\text{Er}$ and $^{28}\text{Si} + ^{154}\text{Sm}$ systems which lead to the same compound nucleus ^{182}Os . The former system serves as a calibration reaction for obtaining the connection between M_γ and $\langle l \rangle$ in the compound nucleus of interest. The use of an electrostatic deflector was crucial to provide the sensitivity needed to make measurements well below the barrier for the latter reaction. The absolute fusion cross sections have also been measured for both systems, providing an important

constraint¹⁹ on the theoretical models used to compare with the experimental $\langle l \rangle$ values. The energy dependence of $\langle l \rangle$ shown in Fig. 2(c) for the $^{28}\text{Si} + ^{154}\text{Sm}$ system demonstrates clearly for the first time the localization in bombarding energy of the large increase in $\langle l \rangle$ expected when the shape degrees of freedom are strongly coupled to the relative-motion degree of freedom.

This work was supported in part by the U.S. Department of Energy, the Comisión Nacional de Energía Atómica (Argentina), the U.S. National Science Foundation, and Consejo Nacional de Investigaciones Científicas y Técnicas (Argentina).

^(a)Permanent address: Instituto de Física da Universidade Federal Fluminense, Niteroi, Brazil.

^(b)Permanent address: Instituto de Física da Universidade de Sao Paulo, Sao Paulo, Brazil.

^(c)Present address: Nuclear Physics Division, Bhabha Atomic Research Centre, Trombay, Bombay 400085, India.

^(d)Present address: Department of Chemistry, Indiana University, Bloomington, IN 47405.

¹M. Beckerman, Phys. Rep. **129**, 145 (1985).

²S. Landowne, in *Proceedings of the Symposium on Heavy Ion Interactions Around the Coulomb Barrier, Legnaro, Italy, 1988*, edited by C. Signorini *et al.* (Springer-Verlag, Berlin, 1988), p. 3.

³S. Gil, R. Vandenbosch, A. Lazzarini, and A. Ray, Phys. Rev. C **31**, 1752 (1985).

⁴R. Vandenbosch, in *Proceedings of the Ninth Workshop in Nuclear Physics, Buenos Aires, Argentina, 1986*, edited by A. Macchiavelli, H. Sofia, and E. Ventura (World Scientific, Singapore, 1987), p. 210.

⁵A. Charlop *et al.*, in *Proceedings of the Symposium on Heavy Ion Interactions Around the Coulomb Barrier, Legnaro, Italy, 1988* (Ref. 2), p. 157.

⁶M. L. Halbert, J. R. Beene, D. C. Hensley, K. Honkanen, T. M. Semkow, V. Abenante, D. G. Sarantites, and Z. Li, Phys. Rev. C **40**, 2558 (1989).

⁷P. J. Nolan *et al.*, Phys. Rev. Lett. **54**, 2211 (1985).

⁸R. G. Stokstad *et al.*, Phys. Rev. Lett. **62**, 399 (1989).

⁹D. E. DiGregorio *et al.*, Phys. Rev. C **42**, 2108 (1990).

¹⁰A. M. Borges *et al.*, in *Proceedings of the Symposium on the Many Facets of Heavy Ions Fusion Reactions, Argonne National Laboratory, March 1986* (unpublished), p. 441.

¹¹R. Vandenbosch *et al.*, Phys. Rev. Lett. **56**, 1234 (1986).

¹²C. H. Dasso and S. Landowne, Phys. Rev. C **32**, 1094 (1985).

¹³D. E. DiGregorio *et al.*, Phys. Rev. C **39**, 516 (1989).

¹⁴J. Fernández Niello *et al.* (to be published).

¹⁵A. Breskin *et al.*, Nucl. Instrum. Methods Phys. Res. **221**, 363 (1984).

¹⁶S. Gil, R. Vandenbosch, A. Charlop, A. García, D. D. Leach, S. J. Luke, and S. Kailas, Phys. Rev. C (to be published).

¹⁷C. Y. Wong, Phys. Rev. Lett. **31**, 766 (1973).

¹⁸J. Fernández Niello, C. H. Dasso, and S. Landowne, Comput. Phys. Commun. **54**, 409 (1989).

¹⁹C. H. Dasso, H. Eshensen, and S. Landowne, Phys. Rev. Lett. **57**, 1498 (1986).